

Simulation of Vibrational Spectra (IR and Raman), PED Analysis and Study of Solvation Effects on Electronic Properties of Methyldopa

Tarun Chaudhary¹, Bhawani Datt Joshi^{2*}

¹Department of Physics, Mid-WEST University, Bageshwary Multiple Campus, Kohalpur, Nepal

²Department of Physics, Tribhuvan University, Siddhanath Science Campus, Mahendranagar, 10400, Nepal

Research Article

©RMC (SNSC), Tribhuvan University

ISSN: 3059-9504 (online)

This work is licensed under the Creative Commons

CC BY-NC License. <https://creativecommons.org/licenses/by-nc/4.0/>

[org/licenses/by-nc/4.0/](https://creativecommons.org/licenses/by-nc/4.0/)

Article History

Received: November 2, 2024

Revised: November 25, 2024

Accepted: December 7, 2024

Published: December 28, 2024

Keywords

IR and Raman, PED, Atomic charge, Charge transfer

*Corresponding author

Email: bhawani.joshi@snsu.edu.np Orcid: 0000-

0003-3276-9319 (BD Joshi)

Phone: + 977-9841580777

ABSTRACT

The properties like hydrogen bonding, partial atomic charges associated with atoms and intramolecular charge transfer characteristics of a drug are very crucial for its biological activity. In the paper, these electronic properties of antihypertensive drug methyldopa have been studied intensively, using Density Functional Theory (DFT). The simulated infrared (IR) and Raman spectra of monomer and dimer, Potential energy distribution (PED), Mullikan atomic charges and UV spectra have been analysed. In both IR and Raman spectra, the prominent stretching of the O-H group taking part in intermolecular hydrogen bonding was obtained at 2814.64 cm⁻¹. Furthermore, the most negative Mulliken charge was found to be associated with nitrogen, N5 and oxygen, O4 and the most positive with carbon atom C10 in monomer. The UV-Vis absorption spectra analysis has been performed in gaseous and solvent (EtOH) states. The present work precisely explains hydrogen bonding, reactive sites and possibility of intramolecular charge transfer.

1. INTRODUCTIONS

The structural and electronic properties of the molecule, which are important factors to determine the chemical and biological properties, have been investigated for a well-known drug, Methyldopa. Methyldopa, (S)-2-amino-3-(3,4-dihydroxyphenyl)-2-methyl-propanoic acid is an antihypertensive drug that has been used since 1960 [1]. It is frequently used to treat preeclampsia and gestational hypertension [2] and preferred for breast-feeding women and often prescribed to heart, kidney, and diabetes patients [3,4]. Methyldopa is more soluble in dimethyl sulfoxide (DMSO) than in water [3].

Methyldopa, being one of the most important and popular medicines, has drawn considerable attention regarding its structural and chemical characteristics. In the last few years, a number of research projects have focused on its structural, thermal, chemical, and biological properties [6-10]. Noei et al. explored the different structure of molecules and their stability due to charge delocalisation in terms of natural bond orbitals (NBO) in different solvents [7]. The previous study shows that the molecule is thermodynamically stable and it exhibits significant non-linear optical properties [6,8]. The molecule shows charge-transfer characteristics with o-chloranil (O-CIN) [9]. Furthermore, Chaudhary et al. showed charge transfer due to excitation based on electron hole distribution [8]. Previously, Prabakaran et al. performed an experimental vibrational study. However, the stretching of frequency of O-H taking part in intermolecular hydrogen bonding remained undetermined. Recently, Chaudhary et al. investigated the structural and chemical properties of the monomer and dimer of methyldopa [10]. However, the analysis of IR and Raman spectra in the monomeric and dimeric forms has not been performed yet. In addition to this, the effects of solvents on their electronic properties are still the subject of interest. Thus, our study is aimed at calculating these properties. As Density Functional Theory (DFT) is an effective method to analyse the structural and electronic properties of the molecules [11], the

overall calculations have been performed using DFT at B3LYP/6-31G(d,p) level of theory. In this paper, IR and Raman spectra of monomer and dimer structures have been simulated and comparatively studied to find out the vibrational shifts of the functional groups taking part in hydrogen bonding. To reproduce the nucleophilic and electrophilic active sites, partial atomic charges associated with the molecule have been calculated. The study of UV-Vis spectra in solvent has been conducted theoretically to get insight into its electronic properties. The present work provides the important information required to understand the molecular reactivity of the molecule more precisely. Fig. 1 depicts the optimized structure of methyldopa dimer.

2. COMPUTATIONAL AND THEORETICAL BACKGROUND

The optimized structure of monomer and dimer of methyldopa were obtained based on previous work of Chaudhry et al. [10] and further calculations were performed using the Gaussian 09 package [12]. The density functional theory (DFT) method [13] with exchange hybrid functional Becke's 3-parameters (Local, nonlocal and Hartree-Fock) and correlation functional Lee-Yang-Parr, B3LYP/6-31G(d,p), was employed for calculations [14-17]. GaussView 05 [18] was used to visualize and analyse the results of Gaussian output. For the vibrational analysis, potential energy distribution (PED) for each of the vibrational modes is obtained using Gar2PED software package [19]. The Raman intensities were calculated utilizing the given equation [20,21]:

$$\frac{\partial \sigma_j}{\partial \Omega} = \left(\frac{2^4 \pi^4}{45} \right) \left(\frac{(v_0 - v_j)^4}{1 - \exp\left[\frac{-hcv_j}{kT}\right]} \right) \left(\frac{h}{8\pi^2 cv_j} \right) S_j$$

where, $\frac{\partial \sigma_j}{\partial \Omega}$ = Raman scattering cross-section,

S_j = scattering activities, v_j = estimated wavenumbers for j^{th} normal mode v_0 = Wave number for the Raman-excited state h , c , and k represent the universal constants. More often, the calculated value of wave numbers is higher than the actual

ones. Thus, the calculated values are adjusted using the WLS factor, $v_{observed} = (1.008700 - 0.0000163 \times v_{calculated}) v_{calculated}$ [22]. Furthermore, Mulliken charges distribution in the

molecule was visualized using GaussView. TD-DFT with integral equation formalism-polarized continuum (IEF-PCM) model was used to analyze UV-Vis spectra.

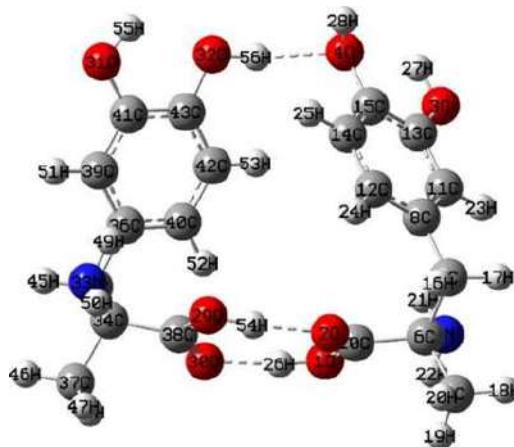


Fig. 1: Optimized structure of methyl dopa dimer at B3LYP/6-311++G (d,p) [10].

3. RESULTS AND DISCUSSIONS

3.1 Vibrational modes

Methyl dopa molecule consists of 28 atoms, so it exhibits 78 vibrational modes. The IR and Raman frequencies for the most stable monomer and dimer are represented in Figs. 2 and 3 respectively. The PED contributions of each of their vibrational modes are illustrated in Table 1. The different vibration modes [23] are explained below:

O-H vibration

Moreover, the stretching of O-H was calculated in between 3530–3645 cm^{-1} [24]. The simulated stretching of the non-bonded O-H group in monomer were observed at 3636.18 cm^{-1} for O4H28, 3583.47 cm^{-1} for O3H27 and 3549.67 cm^{-1} for O1H26. In the dimer, the two hydroxyl groups O4H28 and O3H27 have almost the same frequency as they have in the monomer. However, the stretching frequency of O1H26 was decreased to 2814.64 cm^{-1} . Also, the frequency of hydrogen bonded O-H group of the carboxylic group lies in the range of 3300–2500 cm^{-1} [24]. Hence, the red shift in the frequency of this hydroxyl group justifies the strong hydrogen-bond interaction in the dimer.

NH₂ vibration

The amine group possesses asymmetric and symmetric stretching frequency bands. Its asymmetric stretching was observed at 3403.87 cm^{-1} and symmetric stretching at 3330.73 cm^{-1} in the monomer. Similarly, in the dimer, the asymmetric stretching was obtained at 3399.56 cm^{-1} and symmetric at 3327.20 cm^{-1} . All calculated frequencies lie in the specified range, 3490–3310 cm^{-1} [24]. The strong bending vibration of NH₂ in a plane was determined at 1642.94 cm^{-1} in monomer and 1620.34 cm^{-1} in dimer, respectively. At 874.42 cm^{-1} , the wagging of the monomer has the highest PED contribution.

C-H vibration

The calculated stretching frequency of C-H associated with the ring were obtained at 3071.16, 3065.59, 3030.41 cm^{-1} for the monomer and at 3068.16, 3019.16, 2994.82 cm^{-1} for the dimer structure. These calculated frequencies of C-H are within the range, 3100–3000 cm^{-1} [25, 26]. Furthermore, it's in

plane bending vibration were obtained in the wide range of 1486.0–1127.89 cm^{-1} and out-of-plane bending in 918.49–810.00 cm^{-1} .

The asymmetric stretching of CH₂ was calculated at 2992.55 cm^{-1} and symmetric stretching at 2942.90 cm^{-1} in the monomer. Similarly, its symmetric stretching in dimer was obtained at 2945.81 cm^{-1} . These all calculated frequency bands fall under the given range, that is 3000–2900 cm^{-1} for asymmetric and 2900–2800 cm^{-1} for symmetric [25]. In addition to this, other vibrations occurred intensely at 1464.65 cm^{-1} (deformation), 863.90 cm^{-1} (rocking), 1351.18 cm^{-1} (wagging) and 1259.53 cm^{-1} (scissoring).

The stretching of CH₃ was estimated at 2990.61 cm^{-1} (asymmetric), and at 2924.10 cm^{-1} (symmetric) in the monomer, and 2994.82 cm^{-1} (asymmetric) and 2921.27 (symmetric) in the dimer. The typical range of CH₃ stretching is 3000–2905 cm^{-1} for asymmetric vibrations and 2870–2860 cm^{-1} for symmetric vibrations [27,28]. The deformation of CH₃ with very high contribution PED contribution (87 percent) was calculated at 1393.39 and its rocking were generally obtained below 1127.89 cm^{-1} .

C=O, C-C vibration

The calculated stretching frequency band for C=O in monomer was observed at 1782.40 cm^{-1} , which is in the range, 1870–1550 cm^{-1} [29]. But, in dimer structure, it's frequency was observed at 1723.86 cm^{-1} . This fall in frequency of the carbonyl group, indicates that oxygen is involved in the hydrogen bonding.

The C-C stretching frequencies were almost the same in monomer and dimer. In the monomer, prominent stretching was discovered between 1644.87 cm^{-1} and 1040.80 cm^{-1} . Generally, the stretching frequency bands for C-C lie in between 1650 and 1100 cm^{-1} [30].

Ring vibration

The ring exhibited a variety of vibrations, including puckering, torsional vibration, and trigonal deformation. The considerable puckering of the Ring R was detected at 698.03 cm^{-1} and its asymmetric torsional vibration was found at a very low frequency, 156.03 cm^{-1} .

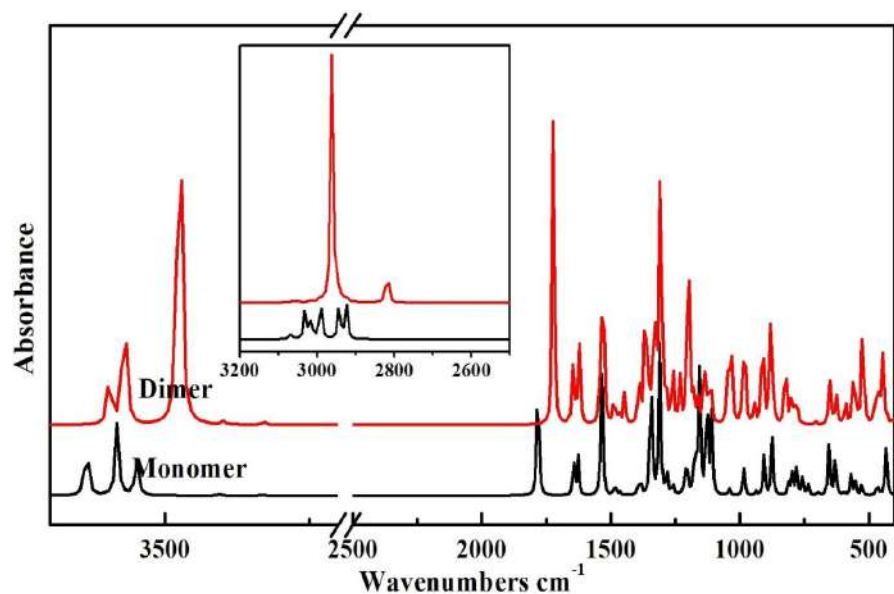


Fig. 2. Simulated IR spectra of methyldopa.

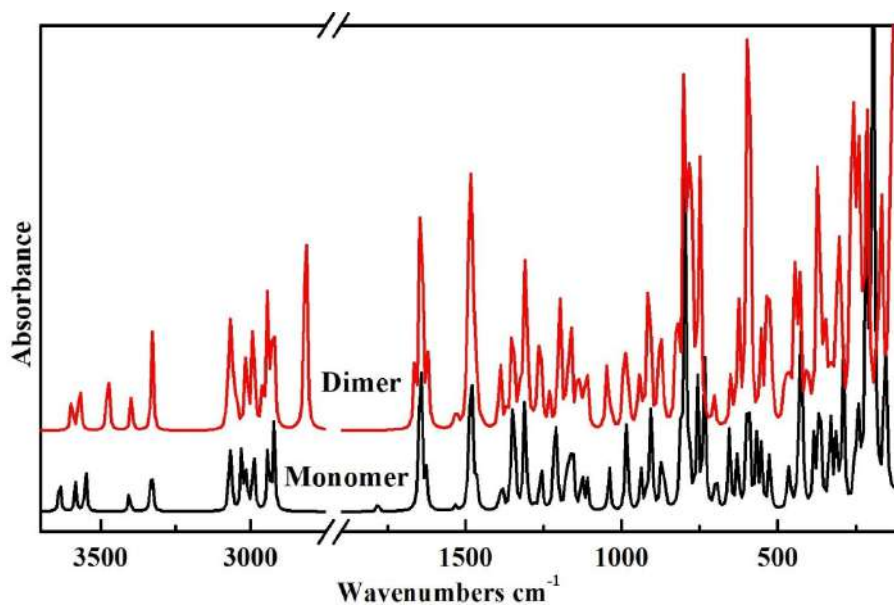


Fig. 3. Simulated Raman spectra of methyldopa.

Table 1. Potential energy distribution (PED) associated with vibrational frequency of methyldopa.

Unscaled frequency	Scaled frequency	IR intensity	Raman activity	PED distribution ($\geq 5\%$)
3843.54	3636.18	69.34	138.30	$\nu(\text{O4H28})(100)$
3783.94	3583.47	88.34	84.77	$\nu(\text{O3H27})(100)$
3745.78	3549.67	48.49	128.48	$\nu(\text{O1H26})(100)$
3581.83	3403.87	2.31	48.09	$\nu_a(\text{NH}_2)(100)$
3499.95	3330.73	2.01	130.34	$\nu_s(\text{NH}_2)(100)$
3211.32	3071.16	1.92	76.14	$\text{R}[\nu(\text{CH})](95)$
3205.60	3065.99	2.01	57.86	$\text{R}[\nu(\text{CH})](98)$
3166.28	3030.41	19.00	98.02	$\text{R}[\nu(\text{CH})](96)$
3149.67	3015.37	12.75	63.38	$\nu(\text{C9H20})(99)$
3124.50	2992.55	5.61	31.26	$\nu_a(\text{CH}_2)(98)$
3122.36	2990.61	20.58	71.92	$\nu_a(\text{CH}_3)(99)$

3069.80	2942.90	22.49	94.36	$v_s(\text{CH}_2)(98)$
3049.12	2924.10	21.37	113.73	$v_s(\text{CH}_3)(99)$
1820.59	1782.40	181.88	2.75	$v(\text{C}=\text{O})(80)+\delta_{in}(\text{C}10\text{H}26)(6)$
1676.08	1644.87	7.92	32.25	$R[v(\text{CC})(45)+\delta_a(10)]$
1674.06	1642.94	41.57	17.45	$\delta_{in}(\text{NH}_2)(87)$
1656.47	1626.16	48.07	7.77	$R[v(\text{CC})(56)+\delta_a'(9)]$
1561.47	1535.31	168.99	1.16	$R[v(\text{CC})(36)+\delta_{in}(\text{CH})(36)+v(\text{C}15\text{O})(9)+v(\text{C}13\text{O})(6)]$
1514.41	1490.20	5.32	10.28	$[\delta_a(45)+\delta_a'(20)+\rho(5)](\text{CH}_3)$
1510.07	1486.04	2.81	9.14	$[\delta_a(18)+\delta_a'(6)](\text{CH}_3)+R[\delta_{in}(\text{C}12\text{H})(11)+v(\text{CC})(30)]+\delta(\text{O}3\text{H})(11)$
1502.99	1479.24	6.99	18.44	$[\delta_a'(57)+\delta_a(23)+\rho'(6)](\text{CH}_3)+\delta(\text{CH}_2)(9)$
1487.79	1464.65	3.58	4.33	$\delta(\text{CH}_2)(85)+\delta_a'(\text{CH}_3)(6)$
1413.67	1393.39	11.55	1.22	$\delta(\text{CH}_3)(87)$
1403.66	1383.76	19.06	5.23	$R[v(\text{CC})(60)]+\delta(\text{O}3\text{H})(9)+\delta(\text{CH}_2)(10)$
1369.85	1351.18	10.89	14.68	$\omega(\text{CH}_2)(40)+\rho(\text{NH}_2)(10)+v(\text{C}6\text{C}9)(6)+\delta(\text{C}8\text{C}6\text{C}7)(6)$
1365.08	1346.58	52.39	1.20	$\delta(\text{C}8\text{C}6\text{C}7)(10)+\delta(\text{O}4\text{H})(9)+v(\text{C}10\text{O})(8)+R[\delta_{in}(\text{CH})(15)]+v(\text{C}6\text{C}10)(7)$
1359.85	1341.54	96.07	7.07	$\delta(\text{O}3\text{H})(16)+R[\delta_{in}(\text{CH})(19)+\delta(\text{O}4\text{H})(8)+\delta(\text{C}8\text{C}6\text{C}7)(8)+v(\text{C}10\text{O})(6)+\omega(\text{CH}_2)(6)]$
1328.81	1311.59	189.62	14.22	$R[v(\text{CC})(33)+\delta_{in}(\text{CH})(7)+v(\text{C}7\text{C}8)(6)+v(\text{C}13\text{O})(21)+v(\text{C}15\text{O})(6)]+\rho(\text{NH}_2)(8)$
1322.28	1305.28	9.79	1.72	$\rho(\text{NH}_2)(28)+\omega(\text{CH}_2)(19)+\delta(\text{C}6\text{C}9\text{N})(8)+\delta'(\text{CH}_3)(6)$
1298.31	1282.13	33.22	0.62	$R[v(\text{C}15\text{O})(17)+\delta_{trig}(15)+\delta_{in}(\text{C}12\text{H})(17)+v(\text{C}13\text{O})(12)]+[\gamma(9)+\omega(7)](\text{CH}_2)+\delta(\text{O}3\text{H})(8)$
1274.93	1259.53	15.97	7.17	$\gamma(\text{CH}_2)(24)+v(\text{N}5\text{C}6)(15)$
1227.59	1213.71	13.78	14.68	$\delta(\text{C}8\text{C}6\text{C}7)(10)+v(\text{N}5\text{C}6)(10)+v(\text{C}6\text{C}7)(9)+v(\text{C}6\text{C}9)(8)+\omega(\text{CH}_2)(7)+\rho(\text{NH}_2)(6)$
1219.71	1206.07	49.87	2.63	$\delta(\text{O}3\text{H})(30)+R[v(\text{CC})(16)+\delta_{in}(\text{CH})(14)+v(\text{C}15\text{O})(6)]+\delta(\text{O}4\text{H})(5)$
1187.41	1174.76	65.78	7.03	$\delta(\text{O}4\text{H})(22)+R[\delta_{in}(\text{CH})(22)+v(\text{C}8\text{C}12)(8)]+v(\text{C}7\text{C}8)(18)$
1174.20	1161.94	16.40	5.20	$R[\delta_{in}(\text{CH})(36)+v(\text{CC})(19)]+\delta(\text{O}4\text{H})(13)+v(\text{C}7\text{C}8)(9)$
1168.26	1156.18	148.73	3.97	$\delta(\text{C}8\text{C}6\text{C}7)(23)+v(\text{C}10\text{O})(22)+\gamma(\text{CH}_2)(14)+v(\text{N}5\text{C}6)(8)$
1139.13	1127.89	144.88	4.82	$\delta(\text{O}4\text{H})(15)+v(\text{C}10\text{O})(11)-R[\delta_{in}(\text{CH})(10)+\delta_{trig}(8)+v(\text{C}15\text{O})(7)]+\rho(\text{CH}_3)(8)$
1120.54	1109.82	100.27	2.96	$\rho(\text{CH}_3)(21)+v(\text{C}10\text{O})(11)+\gamma(\text{CH}_2)(9)+\delta(\text{O}4\text{H})(6)+v(\text{C}8\text{C}11)(6)+R[\delta_{trig}(6)]$
1049.63	1040.80	8.41	4.27	$v(\text{C}6\text{C}9)(25)+\rho'(\text{CH}_3)(22)+\delta(\text{NH}_2)(19)$
992.71	985.28	25.16	6.16	$\rho'(\text{CH}_3)(15)+v(\text{C}6\text{C}7)(12)+v(\text{C}6\text{C}9)(11)+R[v(\text{CC})(7)+v(\text{C}7\text{C}8)(6)+\omega(\text{NH}_2)(6)]$
988.81	981.48	13.18	1.15	$\rho(\text{CH}_2)(26)+\rho'(\text{CH}_3)(17)+\rho(\text{CH}_3)(11)+R[\delta_{trig}(6)]$
945.22	938.88	5.43	3.12	$\omega(\text{NH}_2)(17)+\rho(\text{CH}_2)(13)+\rho(\text{CH}_3)(10)+v(\text{C}6\text{C}9)(8)+R[v(\text{C}8\text{C}12)(7)+\delta_{trig}(7)]$
924.38	918.49	0.98	1.73	$R[\text{oop}(\text{CH})(74)+\tau_a'(6)]$
911.56	905.95	48.85	6.63	$R[\text{oop}(\text{CH})(35)+\text{puck}(6)]+\omega(\text{NH}_2)(20)+v(\text{C}6\text{C}7)(12)$
879.37	874.42	72.00	2.68	$R[\text{oop}(\text{CH})(36)+\omega(\text{NH}_2)(26)+v(\text{N}5\text{C}6)(14)]$
868.64	863.90	2.33	2.80	$v(\text{N}5\text{C}6)(18)+\rho(\text{CH}_2)(16)+R[\text{oop}(\text{CH})(14)+v(\text{C}6\text{C}7)(12)+v(\text{C}6\text{C}10)(9)+\rho(\text{CH}_3)(6)]$
813.71	810.00	19.35	5.21	$R[\text{oop}(\text{CH})(67)+R[\tau_a](8)]$
799.84	796.37	25.84	18.80	$R[v(\text{C}15\text{O})(23)+v(\text{CC})(28)+\delta_{trig}(9)+\delta_a(7)]$
783.91	780.71	31.84	2.08	$\text{oop}(\text{C}10\text{O})(38)+\tau(\text{C}10\text{O})(13)+v(\text{C}6\text{C}9)(11)+R[\text{oop}(\text{C}14\text{H})(6)]$
760.38	757.57	20.88	6.34	$R[\delta_{trig}(16)+\delta_a'(10)+v(\text{C}7\text{C}8)(10)+\text{puck}(6)]+\text{oop}(\text{C}10\text{O})(10)$
737.43	734.98	14.29	7.90	$v(\text{C}6\text{C}10)(19)+\delta_{in}(\text{C}10\text{O})(14)+R[\text{puck}(13)+\text{oop}(\text{C}8\text{C}7)(7)]+v(\text{C}10\text{O})(9)$
699.93	698.03	4.73	2.30	$R[\text{puck}(56)+\text{oop}(\text{C}13\text{O})(14)+\text{oop}(\text{C}15\text{O})(14)+\text{oop}(\text{C}8\text{C}7)(5)]$
656.53	655.22	61.93	3.19	$\tau(\text{C}10\text{O})(28)+R[\text{oop}(\text{C}13\text{O})(16)+\tau_a(10)+\text{oop}(\text{C}15\text{O})(10)+\text{oop}(\text{C}8\text{C}7)(6)]$
630.29	629.30	48.46	2.38	$\tau(\text{C}10\text{O})(26)+R[\tau_a(18)+\text{oop}(\text{C}13\text{O})(13)+\text{oop}(\text{C}8\text{C}7)(13)+\text{oop}(\text{C}15\text{O})(8)]$
596.02	595.41	4.02	6.38	$R[\delta_a'(38)+\delta_{in}(\text{C}15\text{O})(21)+v(\text{CC})(9)+\delta_{in}(\text{C}13\text{O})(6)+v(\text{C}13\text{O})(6)]$
568.84	568.51	25.51	2.34	$\delta_{in}(\text{C}10\text{O})(22)+\delta_a(\text{C}6\text{C}9\text{N})(12)+v(\text{C}6\text{C}10)(9)+\delta(\text{C}6\text{C}10\text{O})(9)+R[\delta_a(6)+\rho'(\text{CH}_3)(6)]$
552.08	551.91	16.19	1.87	$R[\delta_a(12)+\text{puck}(9)+\delta_{in}(\text{C}13\text{O})(8)+\tau_a(7)]+\rho(\text{C}6\text{C}9\text{N})(9)$
526.41	526.47	13.04	1.71	$(\text{C}6\text{C}10\text{O})(17)+\delta(\text{C}6\text{C}9\text{N})(14)+\delta_{in}(\text{C}10\text{O})(12)+\delta_a'(\text{C}6\text{C}9\text{N})(10)+R[\text{puck}(8)]$

Types of vibration: v (stretching), v_a (asymmetric stretching), v_s (symmetric stretching), δ (deformation and bending), oop (out of plane bending), ω (wagging), γ (twisting), ρ (rocking), τ (torsion).

3.2 Mulliken Charge

Atomic charges affect the electronic properties, such as non-linear optical properties and chemical and biological properties of the molecule [31,32]. In addition, it also influences the electronic structure, molecular reactivity, molecular electrostatic potential, etc. [44]. The Mulliken charge associated with each of the atoms is illustrated as shown in Fig. 4. All hydrogen atoms exhibit the positive charges, and all the oxygen and nitrogen atoms exhibit the negative charges. Some carbon exhibits the positive charge,

and some of the carbons exhibit the negative charge. The highest positive charge is associated with carbon atoms C10 and also, the higher negative charges are mainly associated with atoms O4 and N5. The negativity of atom O4 and N5 are also well demonstrated by molecular electrostatic potential (MEP) map in the literature [10]. The positive atoms behave as an electrophilic sites and negative atoms as nucleophilic sites [10, 44]. Thus, these atoms have a crucial role for the non-covalent interactions.

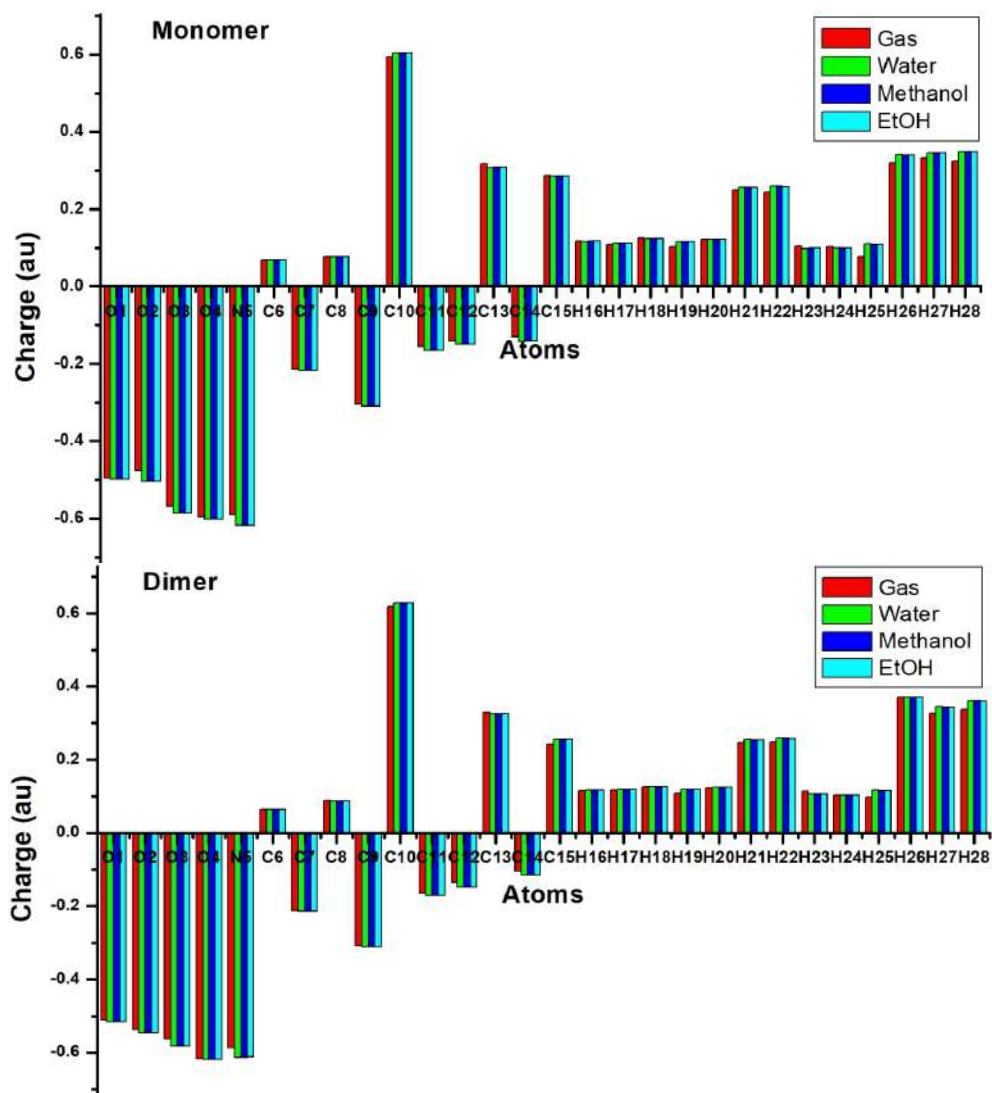


Fig. 4. Mulliken charges associated with each atoms of methyl dopa.

Table 2. Mulliken charges of non-hydrogen atoms of methyl dopa calculated at B3LYP/6-31G(d,p) level of theory.

Monomer				
Atom	Gaseous state	Water e	Methanol e	EtOH e
O1	-0.4947	-0.4980	-0.4980	-0.4980
O2	-0.4777	-0.5050	-0.5042	-0.5038
O3	-0.5699	-0.5873	-0.5868	-0.5865
O4	-0.5957	-0.6021	-0.6019	-0.6018
N5	-0.5911	-0.6193	-0.6184	-0.6179
C6	0.0691	0.0696	0.0696	0.0696
C7	-0.2145	-0.2170	-0.2169	-0.217
C8	0.0770	0.0772	0.0772	0.0772
C9	-0.3054	-0.3093	-0.3093	-0.3093
C10	0.5933	0.6049	0.6045	0.6043
C11	-0.1565	-0.1656	-0.1653	-0.1652
C12	-0.1410	-0.1505	-0.1502	-0.1501
C13	0.3165	0.3070	0.3073	0.3074
C14	-0.1299	-0.1416	-0.1414	-0.1412
C15	0.2869	0.2848	0.2849	0.2850
Dimer (first molecule)				
O1	-0.51149	-0.51602	-0.51591	-0.51585
O2	-0.53638	-0.5458	-0.54553	-0.54538

O3	-0.56245	-0.58205	-0.58148	-0.58118
O4	-0.61617	-0.61831	-0.61835	-0.61836
N5	-0.58676	-0.61375	-0.61284	-0.61237
C6	0.06329	0.06348	0.06348	0.06348
C7	-0.21135	-0.2132	-0.21317	-0.21315
C8	0.08841	0.08753	0.08753	0.08753
C9	-0.30834	-0.31138	-0.31134	-0.31132
C10	0.6186	0.6279	0.62763	0.62749
C11	-0.16531	-0.17131	-0.17112	-0.17103
C12	-0.13475	-0.14843	-0.14786	-0.14758
C13	0.3304	0.32474	0.32485	0.32491
C14	-0.10457	-0.11538	-0.11492	-0.11469
C15	0.24254	0.25723	0.25669	0.25642

3.3 UV-Vis Spectra

The electron transition from the highest occupied molecular orbital (HOMO) to the lowest unoccupied molecular orbital (LUMO) is the main factor that determines the accessibility of chemical reactions, and the energy gap indicates the feasibility of electron transfer [34,35]. In the previous paper [10], the chemical reactivity of the molecule on the basis of the HOMO-LUMO gap has already been discussed. However, the theoretical treatment of the UV-Vis characteristic of the in dimer has not been discussed yet.

The electronic absorption in the bulk of different solvents, TD-DFT with integral equation formalism-polarized continuum (IEF-PCM) model at the same level of theory, has been used

for the computation. Fig. 5 depicts the UV-Vis spectra of methyldopa in a gaseous state and solvent (ethanol). The transitions of electrons in different solvents with their respective excitation energy (ΔE), absorption wavelength (λ) and oscillator strength (f) have been listed in Table 3. In the gaseous phase and in solvent (EtOH), two transition peaks were observed. In gaseous phase, transition peak corresponds to the wavelength 248.82 and 182.91nm (monomer); and 247.34 and 185.78 (dimer). The absorption in solvent, ethanol (EtOH) were observed at 249.4 and 185.78 in monomer and 246.73 and 183.86 nm in dimer. These values were found to be closer to the experimental ones (279, 202 nm) in EtOH [6].

Table 3. Electronic transition properties of methyldopa in the gaseous phase and in solvent.

Gas phase and solvent (EtOH)	Absorption peaks (λ)nm	Oscillator strength (f)	Excitation energy (ΔE) eV	Excitation state
Gas phase	248.82	0.0444	4.9828	HOMO \rightarrow LUMO
	182.91	0.6941	6.7784	HOMO-2 \rightarrow LUMO+2
EtOH	249.4	0.0591	4.9709	HOMO \rightarrow LUMO
	185.78	0.7655	6.6736	HOMO-2 \rightarrow LUMO+2
Dimer				
Gas phase	247.34	0.0638	5.0127	HOMO-1 \rightarrow LUMO
	182.03	0.4951	6.8112	HOMO \rightarrow LUMO+8
EtOH	246.73	0.0918	5.0252	HOMO-1 \rightarrow LUMO
	183.86	1.1861	6.7434	HOMO-5 \rightarrow LUMO+4

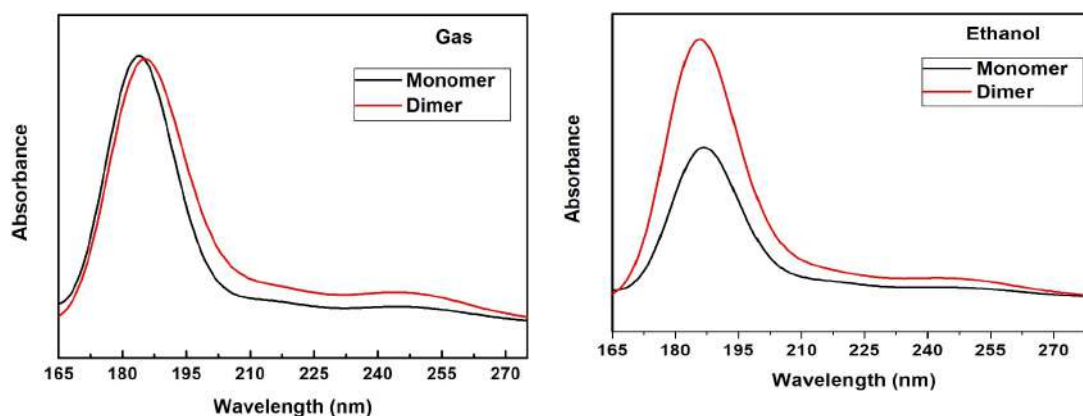


Fig. 5: Simulated UV-Vis absorption spectra for methyldopa in the gaseous phase and in solvent (ethanol).

4. CONCLUSION

The IR and Raman spectra, atomic charge and UV-Vis absorption spectra of methyl dopa have been analysed in the present work. From IR and Raman analysis, functional group, O-H has been justified to from intermolecular hydrogen bonding. Due to the hydrogen bonding, the red shift occurs in the stretching frequency of the O-H group. Thus, the stretching frequency of H-bonded O-H group was explored at 2814.64 cm^{-1} . The Mulliken charge for each of the atoms was calculated. Carbon atoms C10 exhibit the highest positive charge and atoms like O4, N5 exhibit the higher negative charge than others showing higher electrophilic and nucleophilic behavior, respectively. The UV-Vis absorption performed in gaseous phase and in the solvent shows the electronic transition. The intense transition peaks were calculated at 248.82 nm (monomer) and 247.34 nm in (dimer) in the gaseous state, whereas they were found at 249.4 nm (monomer) and 246.73 nm (dimer) in EtOH. Ultimately, the present work provides fundamental and insightful knowledge regarding the intermolecular hydrogen bonding, intramolecular charge-transfer and possible reactive sites which are important for interaction with the target.

ACKNOWLEDGEMENT

We sincerely acknowledge Prof. Poonam Tandon, former HoD, Department of Physics, Lucknow University, India, for providing software facilities, including the Gaussian 09 program.

AUTHOR CONTRIBUTIONS

T. Chaudhary: Writing-original draft, investigation, analysis; and conceptualization; B.D. Joshi: Writing-review, validation and supervision.

CONFLICTS OF INTEREST

There are no conflicts to declare.

REFERENCES

- G.T. Mah, A.M., Tejani, V.M. Musini, Methyl dopa for primary hypertension, *Cochrane Database of Systematic Reviews*, **4** (2009). doi:10.1002/14651858.CD003893
- M. Wicinski, B. Malinowski, O. Puk, M. Socha, M. Stupski, Methyl dopa as an inductor of postpartum depression and maternal blues: A review, *Biomedicine & Pharmacotherapy*, **127** (2020). 110196. doi: 10.1016/j.biopha.2020.110196
- F.H. Amro, H. N. Moussa, O.A. Ashimi, B.M. Sibai, Treatment options for hypertension in pregnancy and puerperium, *Expert Opinion on Drug Safety*, **15** (2016), 1635–1642. doi: 10.1080/14740338.2016.1237500
- M. Noei, M. Holoosadi, H. Anaraki-Ardakani 2017, Design of methyl dopa structure and calculation of its properties by quantum mechanics, *Arabian Journal of Chemistry*, **10** (2017) S1923–S1937. doi: 10.1016/j.arabjc.2013.07.021
- K. Sharma, S. Sharma, S. Lahiri, Spectrophotometric, fourier transform infrared spectroscopic and theoretical studies of the charge-transfer complexes between methyl dopa [(s)-2 amino-3-(3, 4-dihydroxyphenyl)-2-methyl propanoic acid] and the acceptors (chloranilic acid, o-chloranil and dichlorodicyanobenzoquinone) in acetonitrile and their thermodynamic properties, *Spectrochimica Acta Part A: Molecular and Biomolecular Spectroscopy*, **92** (2012) 212–224. doi: 10.1016/j.saa.2012.02.072
- A. Prabakaran, S. Muthu, Normal coordinate analysis and vibrational spectroscopy (FT-IR and FT-Raman) studies of (2S)-2-amino-3-(3, 4-dihydroxyphenyl)-2-methylpropanoic acid using ab initio HF and DFT method, *Spectrochimica Acta A Molecular and Biomolecular Spectroscopy*, **99** (2012) 90-96. <https://doi.org/10.1016/j.saa.2012.09.014>
- M. Noei, M. Holoosadi, H. Anaraki-Ardakani, Design of methyl dopa structure and calculation of its properties by quantum mechanics, *Arabian Journal of Chemistry*, **10** (2017) S1923-S1937. <https://doi.org/10.1016/j.arabjc.2013.07.021>
- T. Chaudhary, M.K. Chaudhary, B.D. Joshi, A theoretical study on charge transfer and hyperpolarizability of (s)-2-amino-3-(3, 4-dihydroxyphenyl)-2methyl-propanoic acid, *Journal of Nepal Physical Society*, **8** (2022), 16–21. <http://doi:10.3126/inphysoc.v8i1.48280>
- D.A. Ostrov, A. Alkanani, K.A. McDaniel, S. Case, E.E. Baschal, L. Pyle, . . . others, Methyl dopa blocks MHC class II binding to disease-specific antigens in autoimmune diabetes, *The Journal of clinical investigation*, **128** (2018), 1888–1902. doi: 10.1172/jci97739
- T. Chaudhary, T. Karthick, M.K. Chaudhary, P. Tandon, B.D. Joshi, Computational evaluation on molecular stability and binding affinity of methyl dopa against lysine-specific demethylase 4d enzyme through quantum chemical computations and molecular docking analysis, *Journal of Molecular Structure*, **1286** (2023) 135518. doi: 10.1016/j.molstruc.2023.135518
- T. Chaudhary, M.K. Chaudhary, S. Jain, P. Tandon, B.D. Joshi, The experimental and theoretical spectroscopic elucidation of molecular structure, electronic properties, thermal analysis, biological evaluation, and molecular docking studies of isococculidine, *Journal of Molecular Liquids*, **391** (2023) 123212. <https://doi.org/10.1016/j.molliq.2023.123212>
- M.J. Frisch, G.W. Trucks, H.B. Schlegel, G.E. Scuseria, J.R. Cheeseman, M.A. Robb, G. Scalmani, V. Barone, B. Mennucci, G.A. Petersson, H. Nakatsuji, M. Caricato, X. Li, H.P. Hratchian, A.F. Izmaylov, J. Bloino, G. Zheng, J.L. Sonnenberg, M. Hada, M. Ehara, K. Toyota, R. Fukuda, J. Ishida, M. Hasegawa, T. Nakajima, Y. Honda, O. Kitao, H. Nakai, T. Vreven, J.A. Montgomery Jr., J.E. Peralta, F. Ogliaro, M. Bearpark, J.J. Heyd, E. Brothers, K.N. Kudin, V.N. Staroverov, R. Kobayashi, J. Normand, A. Raghavachari, A. Rendell, J.C. Burant, S.S. Iyengar, J. Tomasi, M. Cossi, N. Rega, J.M. Millam, M. Klene, J.E. Knox, J.B. Cross, V. Bakken, C. Adamo, J. Jaramillo, R. Gomperts, R.E. Stratmann, O. Yazyev, A.J. Austin, R. Cammi, C. Pomelli, J.W. Ochterski, R.L. Martin, K. Morokuma, V.G. Zakrzewski, G.A. Voth, P. Salvador, J.J. Dannerberg, S. Dapprich, A.D. Daniels, J. Farkas, B. Foresman, J.V. Ortiz, J. Cioslowski, D.J. Fox, Gaussian 09, Revision, Gaussian, Inc., Wallingford CT, 2009.
- P. Hohenberg, W. Kohn, Inhomogeneous Electron Gas, *Physical Review B*, **136** (1964) 864–871. <http://dx.doi.org/10.1103/PhysRev.136.B864>
- C. Lee, W. Yang, R.G. Parr, Development of the Colle-Salvetti correlation-energy formula into a functional of the electron density, *Physical Review B*, **37** (1998) 785-789. <https://doi.org/10.1103/PhysRevB.37.785-789>
- R.G. Parr, W. Yang, Density Functional Theory of Atoms and Molecules, Oxford University Press, New York, 1989 1-325

- [16] A.D. Becke, Densityfunctional thermochemistry III, The role of exact exchange, *The Journal of Chemical Physics*, **98** (1993) 5648–5652. <http://dx.doi.org/10.1063/1.464913>
- [17] T.H. Dunning Jr, Gaussian basis sets for use in correlated molecular calculations. I. The atoms boron through neon and hydrogen, *The Journal of Chemical Physics*, **90** (1989) 1007–1023. <https://doi.org/10.1063/1.456153>
- [18] A. Frisch, A.B. Nielson, A.J. Holder, GaussView User Manual, Gaussian Inc, Pittsburgh, PA (2005).
- [19] J.M.L. Martin, C. Van Alsenoy, Gar2ped, “Gar2ped software.” University of Antwerp (1995).
- [20] P. L. Polavarapu, Ab initio vibrational Raman and Raman optical activity spectra, *The Journal of Physical Chemistry*, **94** (1990) 8106–8112. doi: [10.1021/j100384a024](https://doi.org/10.1021/j100384a024)
- [21] G.A. Guirgis, P. Klaboe, Shen, S. Powell, D L. Gruodis, A.V. Aleksa, J.R. Durig, (2003). Spectra and structure of silicon-containing compounds. xxxvi—raman and infrared spectra, conformational stability, ab initio calculations and vibrational assignment of ethyldibromosilane, *Journal of Raman Spectroscopy*, **34** (2003), 322–336. doi: [10.1002/jrs.989](https://doi.org/10.1002/jrs.989)
- [22] H. Yoshida, K. Takeda, J. Okamura, A. Ehara, H. Matsuura, A new approach to vibrational analysis of large molecules by density functional theory: wavenumber-linear scaling method, *The Journal of Physical Chemistry A*, **106** (2002) 3580–3586, doi: [10.1021/jp013084m](https://doi.org/10.1021/jp013084m)
- [23] T. Chaudhary, Structural and spectroscopic studies on cefalexin and methyl dopa using quantum mechanical methods (Unpublished Ph.D. Thesis, Central department of Physics, Tribhuvan University, Nepal) 2024.
- [24] J. Coates, Interpretation of infrared spectra, a practical approach, *Encyclopedia of analytical chemistry*, **12** (2006), 815–10. doi: [10.1002/9780470027318.a5606](https://doi.org/10.1002/9780470027318.a5606)
- [25] S. Muthu, J.U. Maheswari, Quantum mechanical study and spectroscopic (FT-IR, FT-Raman, 13C, 1H, UV) study, first order hyperpolarizability, NBO analysis, HOMO and LUMO analysis of 4-[(4-aminobenzene) sulfonyl] aniline by ab initio HF and density functional method, *Spectrochimica Acta Part A: Molecular and Biomolecular Spectroscopy*, **92** (2012)154–163. doi: [10.1016/j.saa.2012.02.056](https://doi.org/10.1016/j.saa.2012.02.056)
- [26] S. Sevvanthi, S. Muthu, M. Raja, Quantum mechanical, spectroscopic studies and molecular docking analysis on 5, 5-diphenylimidazolidine-2, 4-dione, *Journal of Molecular Structure*, **1149** (2017) 487–498. doi: [10.1016/j.molstruc.2017.08.015](https://doi.org/10.1016/j.molstruc.2017.08.015)
- [27] C. Liu, R. Alfano, W. Sha, H. Zhu, D. Akins, J. Cleary, . . . E. Cellmer, Human breast tissues studied by ir fourier-transform raman spectroscopy, *In Conference on lasers and electro-optics* (1991) p. CWF51. <https://opg.optica.org/abstract.cfm?uri=cleo-1991-CWF51>
- [28] N.L. Alpert, W. E. Keiser, H.A. Szymanski, N.L. Alpert, W.E. Keiser, H.A. Szymanski, Instruments, *IR: Theory and Practice of Infrared Spectroscopy*, (1979) 9–64. doi: [10.1007/978-1-4684-8160-0_2](https://doi.org/10.1007/978-1-4684-8160-0_2)
- [29] G. Socrates, *Infrared and raman characteristic group frequencies: tables and charts*, John Wiley & Sons, 2004. Retrieved from <http://surl.li/lkfpl>
- [30] A. Srivastava, T. Karthick, B.D. Joshi, R. Mishra, P. Tandon, A. Ayala, J. Ellena, Spectroscopic (far or terahertz, mid-infrared and raman) investigation, thermal analysis and biological activity of piplartine. *Spectrochimica Acta Part A: Molecular and Biomolecular Spectroscopy*, **184** (2017) 368–381. doi: [10.1016/j.saa.2017.05.007](https://doi.org/10.1016/j.saa.2017.05.007)
- [31] P.L. Polavarapu, Ab initio vibrational raman and raman optical activity spectra, *Journal of Physical Chemistry*, **94** (1990) 8106–8112, <https://doi.org/10.1021/j100384a024>
- [32] S. Muthu, J.U. Maheswari, Quantum mechanical study and spectroscopic (FT-IR, FT-Raman, 13C, 1H, UV) study, first order hyperpolarizability, NBO analysis, HOMO and LUMO analysis of 4-[(4-aminobenzene) sulfonyl] aniline by ab initio HF and density functional method, *Spectrochimica Acta A Molecular and Biomolecular Spectroscopy*, **92** (2012) 154–163, <https://doi.org/10.1016/j.saa.2012.02.056>
- [33] G.A. Guirgis, P. Klaboe, S. Shen, D.L. Powell, A. Gruodis, V. Aleksa, C.J. Nielsen, J. Tao, C. Zheng, J.R. Durig, Spectra and structure of silicon-containing compounds. XXXVI—Raman and infrared spectra, conformational stability, ab initio calculations and vibrational assignment of ethyldibromosilane, *Journal of Raman Spectroscopy*, **34** (2003) 322–336, <https://doi.org/10.1002/jrs.989>.
- [34] B.D. Joshi, A. Srivastava, P. Tandon, S. Jain, A.P. Ayala, A combined experimental (IR, Raman and UV–Vis) and quantum chemical study of canadine, *Spectrochimica Acta A: Molecular and Biomolecular Spectroscopy* **191** (2018) 249-258. <https://doi.org/10.1016/j.saa.2017.10.008>
- [35] N.N. Ayare, V.K. Shukla, N. Sekar, Charge transfer and nonlinear optical properties of anthraquinone D- π -A dyes in relation with the DFT based molecular descriptors and perturbational potential, *Computational and Theoretical Chemistry*, **1174** (2020) 112712. <https://doi.org/10.1016/j.comptc.2020.112712>